

Mechanism of electron beam radiation damage on carbon nanofiber surface

M.C. Evora ^{1,2}, D. Klosterman ², K. Lafdi ², L. Li, L. G. A. Silva ³

1 Instituto de Estudos Avançados (Institute for Advanced Studies), São Jose dos Campos-SP/ Brazil.

2 Chemical & Materials Engineering, University of Dayton, Dayton, Ohio 45469-0246.

3 Instituto de Pesquisas Energéticas e Nucleares (IPEN/CNEN-SP) Av. Prof. Lineu Prestes, 2242, Cidade Universitária, 05508-000 –SP/ Brazil.

Key words: Carbon nanofibers, electron beam, oxidation.

Email address: cecilia@ieav.cta.br

This study explored the use of a high energy electron beam as the only available technique for selective area surface modification of carbon nanofibers through controlled parameters such as radiation dose, sample temperature, and environment. The application of this variable space led to the production of unique morphological features on the nanofiber surfaces. Transmission Electron Microscopy was used to allow direct observation of carbon structures undergoing electron beam irradiation and establish the mechanism for these surface modifications. Depending on the exposure parameters, a nanofiber surface rich with some or all of the following was created: i) free radicals, ii) chemisorbed or physisorbed functional groups, iii) surface roughness from peeling and recombination of graphene layers, and iv) activated carbon surface with nano to meso porosity. To further understand the structural changes of irradiated carbon nanofibers, WAXD analysis was performed on non irradiated and irradiated samples. There is a considerable expansion of the lattice in the irradiated samples leading to an increase of interplanar spacing (d spacing). The demonstrated consequences of these selective modifications were improved dispersion of the nanofibers in liquid and good bonding with epoxy.

1. Introduction

The effect of ionizing radiation on carbon materials takes place as a displacement of carbon atoms from their amorphous or graphitic structures. For nanocarbon materials, only destructive effects were observed in early experiments involving bombardment of carbon nanotubes and fullerenes with ions. However, recent work reveals that radiation can exploit defect creation for novel materials development especially in electronic nanotechnology¹.

It is known that electron beam can be used to mechanically manipulate the interconnection of carbon nanostructures at high temperatures using TEM. For example, two crossing pristine tubes would not normally join, even at high temperatures, cutting, welding and transform local arrangements of single wall tubes to multiwall tubes². The stability of nanotubes under electron irradiation is governed by generation and annealing of vacancies-interstitials pair. The interstitial defects have higher mobility and

will determine the annealing process. Agglomeration of vacancies will lead the radiation cutting³. Also, radiation induces vacancies, and the energy gain by dangling bond saturation can weld both tubes as well as react with oxygen. It can be a good contribution in nano-electronic structure because it may improve the electric conductivity for example. Previous studies had shown that making an electrically conductive connection between nanotubes is not straightforward. Instead of the desirable ohmic contacts, tunnel junctions are often generated with high resistance⁴⁻⁷. For example, at high temperature a focused electron beam in a field emission transmission electron microscope (TEM) was able to transform local arrangements of single wall tubes to multiwall tubes². Plegler et al. used computational molecular dynamic simulation to study electron beam modification of MWNT. They concluded that electron beam is not surface limited and may lead to cross-links between inner layers⁸.

Carbon nanofibers are being thoroughly investigated for application in structural composites for in the aerospace industry. This will require careful control of the surface to promote properties required for end use because CNFs are not highly compatible with most polymers. Therefore, it is necessary to modify their surfaces through chemical or physical techniques to produce optimized polymer nanocomposites. Oxidizing the nanocarbon surface creates active sites, changing non polar sites to polar compounds that are available for further chemical reaction or “grafting” (chemical reaction) with additional organic groups. Graphitic nanostructures show a variety of structural transformations under electron irradiation such as accumulation of defects rearrangement to new morphologies with desirable properties. The goal of the present study is to investigate the mechanism of electron beam radiation damage on carbon nanofiber surface to understand structural changes on irradiated carbon nanofibers.

To this end, CNF samples were exposed to electron beam facility at high levels of e-beam radiation doses in an atmosphere of air. Wide angle X ray diffraction analysis (WAXD) was performed on non irradiated and irradiated samples. This technique was used to investigate the topography of a material at the atomic level and it is more sensitive to the atomic and molecular features below the nanometer dimension⁹. Transmission Electron Microscopy was used to allow direct observation of carbon structures undergoing electron beam irradiation and establish the mechanism for these surface modifications.

2. Experimental

Pyrograf III™ Vapor Grown Carbon Nanofibers (VGCFs) were purchased from Applied Sciences Inc. (Cedarville, Ohio). Several grades of VGCFs are available, which differ in bulk density, wall architecture, overall diameter, and prior heat treatment. We selected the PR-25-PS-XT grade, which has an average diameter of 80 nm and has been heat treated in an inert atmosphere up to 1100°C to remove polyaromatic hydrocarbons and metal catalyst impurities from the surface. This grade has a good balance of mechanical and electrical properties. The as-received material was in the form of a loose powder with bulk density of approximately 0.032 g/cm³. Compared to other grades of Pyrograf III, such as PR-24 and PR-19, the PR-25 grade has lower iron content, a smaller diameter, and a larger number of graphitic edge sites available along the length.

The Transmission Electron Microscope (TEM) used in this research was a Tecnai F20 system with a field emission 200kV S/TEM with an X-TWIN lens. This lens allowed a 30 degree tilt with a low background double tilt holder, and allowed ± 70 degrees of tilt with the tomography holder. TEM was used to study the electron beam radiation process on PR-25-PS. TEM images were collected with real

time dynamics using a focused electron beam and a charged coupled device (CCD) camera that converted optical brightness into electrical amplitude. With these images it was possible to explain what happens in real time when the electron beam heats the surface of the samples.

As-received PR-25-PS-XT was also irradiated with a direct accelerator operated by the E-BEAM Services Inc. (Lebanon, Ohio, USA). Samples, as a loose powder, were placed on a steel platform below a linear scan horn. The samples were irradiated with a 150kW Dynamitron manufactured by RDI (Radiation Dynamics Inc.) This equipment is a DC potential drop accelerator that was operated with the following parameters: beam energy 4.5 MeV, dose rate 15.7 kGy/sec, dose history: 25 kGy/pass for 10 passes, 20 kGy/pass for 37 passes, 10 kGy/pass for 1 pass for a total dose of 1000 kGy (where 1 kGy = 1kJ absorbed energy / kg material = 0.1 Mrad). Samples were irradiated in air by placing loose powder in an aluminum pan (21.5 cm x 11.5 cm x 6 cm) to a depth of 4 cm. Another sample was irradiated in vacuum using a Mylar vacuum bag evacuated to about 25-25.5 in Hg of vacuum. The vacuum and open-air sample was irradiated at the same time one next to another.

The structural changes of irradiated carbon nanofibers were investigated by WAXD analysis performed on non irradiated and irradiated samples. The X-ray diffractometer used on this study is a Rigaku Ultima III model with Cu/K-alpha radiation (wavelength 1.54059 Å). The X-ray tube was operated at 40 KV, 40 mA.

3. Results and discussion

3.1- Mechanism of radiation damage on carbon nanofiber PR-25-PS surface

In addition to providing information about the mechanism of radiation damage on carbon nanofiber PR-25-PS surface, TEM was used to allow direct observation of carbon structures undergoing electron beam irradiation. The aim of this TEM analysis was to understand the effect of electron beam radiation on the structure of the carbon nanofiber and understand how the nature of oxygen functional groups attached to the carbon nanofiber surface.

Dislocations, dangling bonds, and electronic excitations are the most important radiation effects on nanocarbon structures. All these effects may be related to the capacity of nanocarbon structures to react with heteroatoms, self heal and rearrange themselves by going through a recombination process. The recombination of interstitials and vacancies is expected to be the primary step in Wigner energy release which is stored in the interstitial when the atom is dislocated at this position and is liberated posterior recombination process¹⁰.

The carbon nanofiber has a very organized core and is cover with a thin layer of turbostratic carbon. This turbostratic layer is a less organized external layer of carbon, is less resistant to radiation, and is the layer that will receive the primary knock on.

As shown in Figure 1, when the electrons hit the turbostratic layer, a fog of free radicals is created that it is very sensitive to the environment. The TEM was carried out in vacuum but in the regular experiment, the samples were irradiated in air. The oxygen of the air dissociates in ozone

molecules when interacts with electron beam. These ozone molecules are very reactive and were present in the atmosphere around the samples undergoing irradiated¹¹.

Depending on the amount of energy involved in the process (considering primary and secondary electrons from the cascade effect), defects (dangling bonds, vacancies, interstitial, pentagon-heptagon pair defects) are created in the graphene structure, and a high strain at the sites of defects should be considered. With defects expanding, the increased tensile force leads to a less stable structure compared with perfect hexagonal carbon network. The continuous electron beam heating may easily break C-C bonds from defects, causing carbon atom sublimation (see Figure 1) and further evaporation of a graphene fragment¹². The sublimed carbon may also recombine to form a new arrangement leading to some reactions with oxygen available in the vault. The damage process is present, however it is not sufficiently intense to damage the core of the PR-25-PS and this may explain Raman curves presented in¹¹. Adding to oxidation, welding of two carbon nanofibers can be possible because the deposition of amorphous carbon¹².

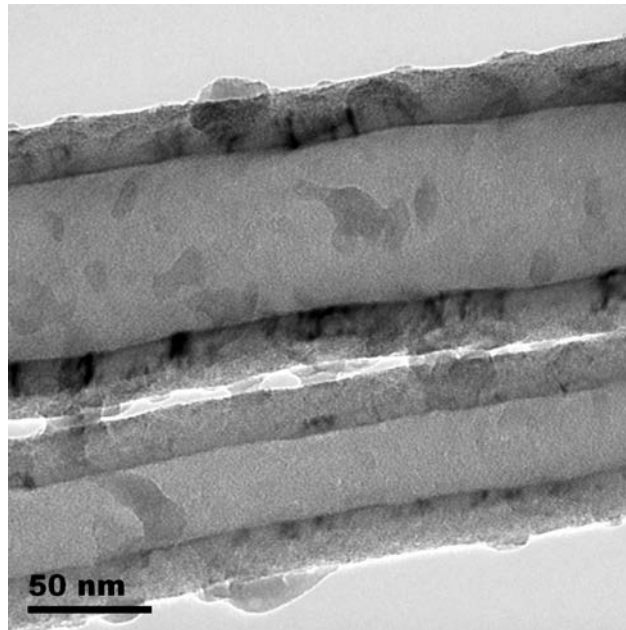


Figure 1: Evidence of fog of free radical formed after radiation with electron beam from TEM.

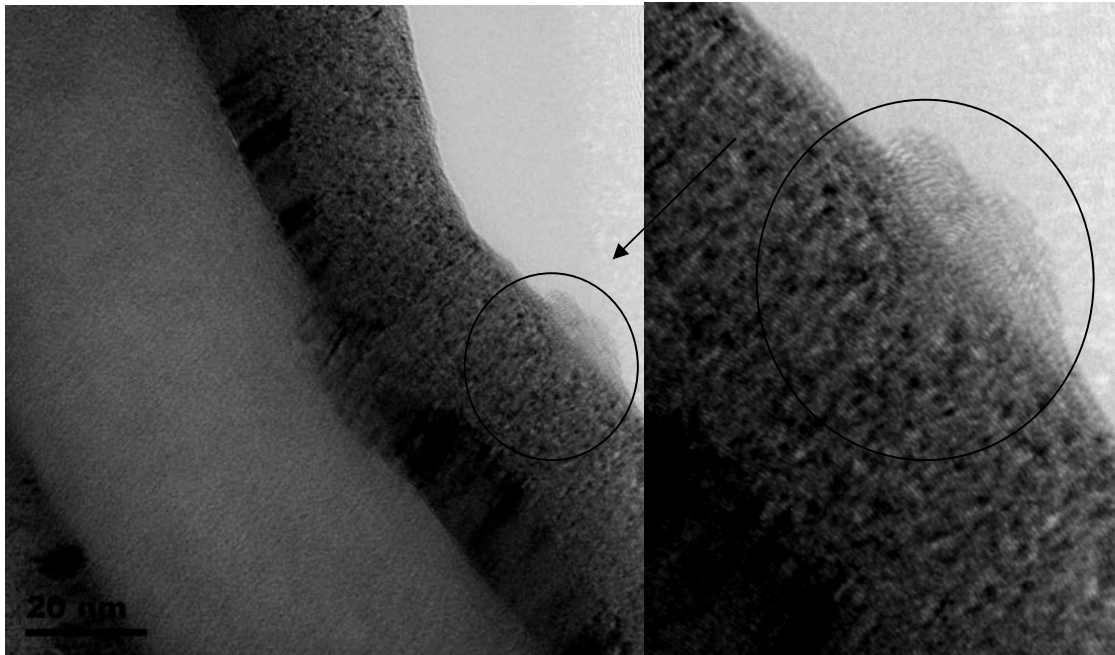


Figure 2: Recombined carbon in the form of curling graphitic flakes (in the circles) and a typical point of defect where the carbon nanofiber may be cut.

Figure 2 is a high magnification image of the recombination after carbon evaporation under the beam. Curled graphitic flakes exhibiting a wave-like structure with random twist are formed. They appear as a carbon onion structure in a combination of SW defects known as pentagon and heptagon carbon rings. There will be nucleation sites for growing curved graphitic flakes¹³. The 3 different types of graphitic carbon rings are illustrated in Figure 3.

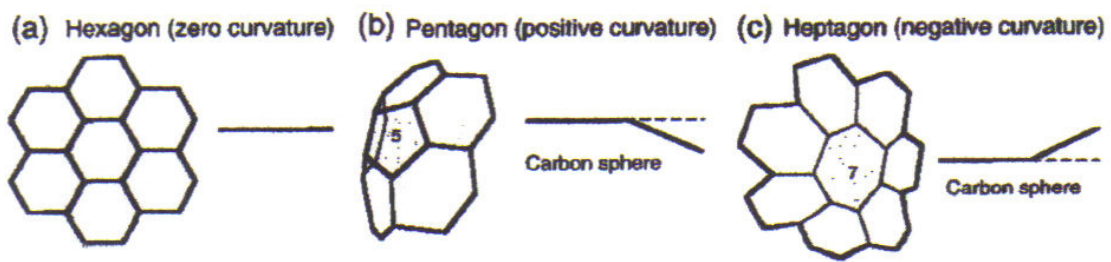


Figure 3: (a) Hexagon, (b) Pentagon (a) Heptagon carbon ring structure in graphitic flakes¹³

There is also an indication of cutting process in PR- 25- PS presented in Figure 4 and it is indicated by the arrow. The outer shell narrowed slightly, which may be a precursor to cutting site. Also, and a crack is present with migration of interstitials to the inner shell.

Figure 4 is an example of cutting by electron beam because the accumulation of vacancies breaks the side wall of PR-25-PS. In Figure 5, a high magnification image of a cutting site is indicated by white arrow. There is a formation of a very organized graphene layers in very well defined whorl format.

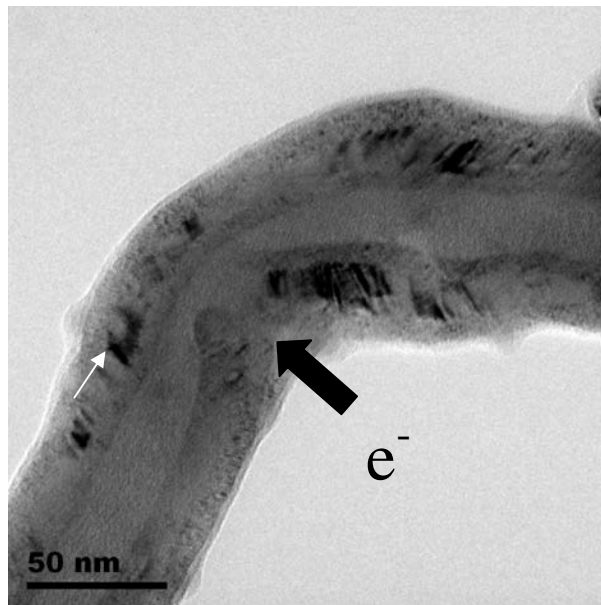


Figure 4: TEM image showing accumulation of vacancies due to irradiation with electron beam from TEM resulting break in the fiber wall.

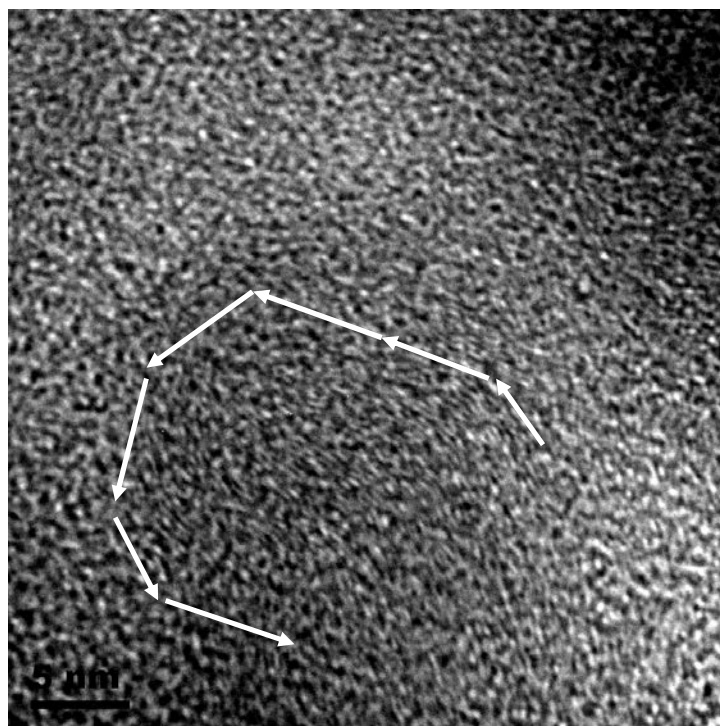


Figure 5: TEM image showing formation of whorl pattern at the site indicated by the white arrow after irradiation with electron beam.

3.2 X Ray diffraction

To further understand the structural changes of irradiated PR-25-PS in air, a WAXD analysis was performed on non irradiated and irradiated samples. The results indicate that the material posses two phases. There is a difference in intensity between the XRD patterns of the carbon nanofiber non irradiated and irradiated at 1000 kGy in vacuum (see Figure 6) and it is an indication that the radiation promote modification on the carbon nanofiber surface. In addition, there is a considerable expansion of the lattice in the irradiated samples leading to an increase of interplanar spacing (d spacing). It is important to point out the increase of d spacing of the sample irradiated in vacuum to 1000 kGy compared to the non irradiated sample and sample irradiated in air to 1000 kGy (see Table 1). This result confirms that the carbon nanofiber structure is modified from radiation even under vacuum. The XRD results are in good agreement with HTEM results presented in Section 4.9. The oxygen attached on the surface due to reaction with free radical generated by electron beam process may also contribute to increase of d spacing. Zhang et al. also observed that nitric acid oxidation of SWNT films led to an increase in the d spacing¹⁴.

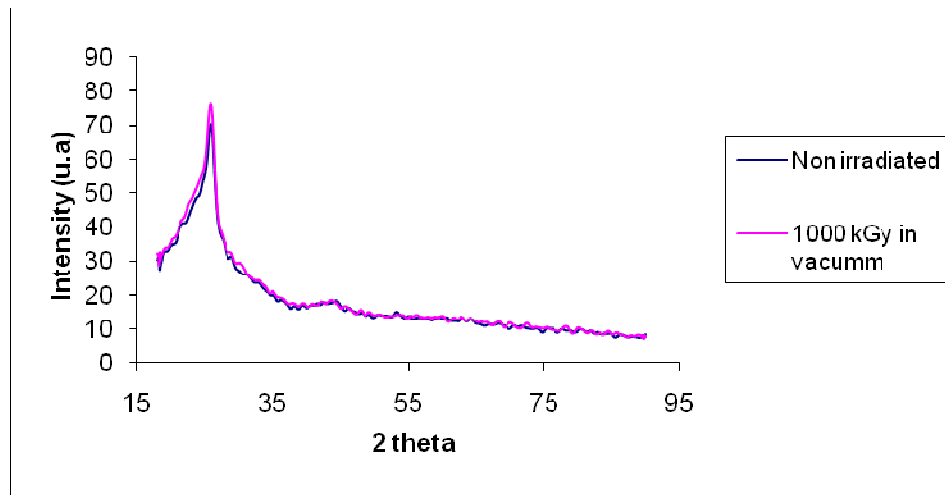


Figure 6: WAXD Patterns for samples non irradiated and irradiated at 1000 kGy dose in vacuum.

Table 1: d spacing results of non irradiated and irradiated PR-25-PS.

| Sample | d phase 1 (nm) | d phase 2 (nm) |
|-------------------|----------------|----------------|
| Non irradiated | 0.37396 | 0.34140 |
| 1000 kGy/air | 0.37624 | 0.34153 |
| 1000 kGy / vacuum | 0.38278 | 0.34409 |

XRD is important analysis to investigate changes material structure. Endo et al investigated the structural changes in stacked cup carbon nanofibers by heat treatment from 1800 to 3000°C. The increased value of the interlayer spacing for samples at 1800°C was attributed to structural disruption at graphene edge planes during the formation of single loops and transformation into multiple loops¹⁵. The crystallite size were calculated using the Scherrer Equation

$$L = k\lambda / (B \cos \theta)$$

where $k = 0.9$ (for L_c) and $k = 1.84$ (L_a), $\lambda = 0.154059$ (for Cu target).

This method is the classical way to determine the dimensions of small crystals using three dimensional reflections of appropriated indices such as (002) and (100)¹⁶⁻¹⁷.

The L_c represents a measure of the average stacking height of the layers, and it is widely known that L_c is a function of crystallinity¹⁸. The value of L_a represents the diameter of the crystal as shown in Figure 7. The results of crystallite size are presented in Table 2. L_c and L_a decrease after the samples were irradiated. L_c and L_a represent the distance between defects, and the results show that these distances decrease due to the generation of more defects. This relationship of decreasing defect distance and increasing number of defects is consistent with TEM images.

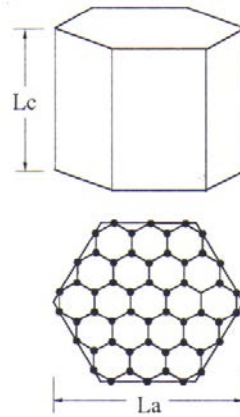


Figure 7: Crystallite shape of graphite crystal¹⁹.

Table 2: Crystallite size of non irradiated and irradiated PR-25-PS.

| Sample | Lc - phase 1 (nm) | Lc - phase 2 (nm) | La (nm) |
|-------------------|-------------------|-------------------|---------|
| Non irradiated | 2.07442 | 5.60564 | 7.21654 |
| 1000 kGy/air | 1.64275 | 5.19162 | 5.51286 |
| 1000 kGy / vaccum | 1.41707 | 3.97782 | 5.47998 |

4. Conclusion

The results presented in this study represent a step toward understanding the effect of e-beam radiation on carbon nanofiber surfaces and an alternative way to modify the surface of nanofibers through controlled parameters such as power of exposure, temperature, time, and environment. Application of this unique variable space gives the user custom control over the surface interaction with other media. Analytical techniques such as TEM and X-ray diffraction were used to establish the

mechanism for these surface modifications. A nanofiber surface rich with some or all of the following features can be produced:

- i) In all environments, free radicals are created on the nanofiber surface by e-beam knock-on damage which leads to vacancies and other point defects. These produce a very energetic surface that enhances bonding with polar media.
- ii) If an environment is present such as oxygen, the energy and power of the beam will determine if the gas molecules will also become ionized and chemisorbed on the surface, or remain unionized and physisorbed on the surface.
- iii) Another effect of the beam power is the peeling of poorly bonded basic structural units, followed by their recombination to produce a surface roughness at the nano scale.
- iv) When the e-beam interacts with the carbon structure in an oxidative environment (O_2 , H_2O), the carbon surface oxidizes to CO and CO_2 . At high temperature these reactive gasses lead to an activated carbon surface with nano to meso porosity.

The mechanism for these effects was elucidated through use of high resolution TEM. The carbon structures were observed directly while undergoing electron beam irradiation. When the electrons hit the turbostratic layer, a fog of free radicals was created that was very sensitive to the environment. The accumulation of defects and damage led to an increase of interlayer spacing between graphene layers and a reduction in the grain size of the crystallites.

Acknowledgements

The authors wish to thank Capes/Fulbright for Ms. Evora fellowship and Applied Science Inc. for providing the carbon nanofiber. Finally the author would like to thank Mr Czarnecki for the X ray diffraction analysis and Mr Dave Keenan from E-BEAM Services.

References

1. Krashennikov AV, Banhart F. Engineering of nanostructured carbon materials with electron or ion beams. *Nature Materials* 2007; 6: 723-33.
2. Li J, Banhart F. The engineering of hot carbon nanotubes with a focused electron beam, *Nano Letters* 2004; 4, n 6: 1143-46.
3. Banhart F, Jixue L, Terrones M. Cutting Single-Walled Carbon Nanotubes with an electron beam: Evidence for atom migration inside nanotubes. *Small Journal* 2005; 1, n. 10: 953-56.
4. Gupta S, Patel RJ, Smith ND. Advanced Carbon-based materials as space radiation shield. *Mater. Res. Soc. Symp. Proc.* 2005; 851:1-7.
5. Krashennikov AV, Banhart F. Engineering of nanostructured carbon materials with electron or ion beams. *Nature Materials* 2007; 6: 723-33.
6. Zou H, Yang Y, Li Q, Zhang J, Liu Z. Electron beam- induced structure transformation of single-walled carbon nanotubes. *Carbon* 2002; 40: 2263-84.
7. Elektronenmikroskopie Z E. The formation of connection between carbon nanotubes in an electron beam. *Nano Lett* 2001; 1, n 6: 329-32.
8. Pregler SK, Sinnott SB. Molecular dynamics simulations of electron and ion beam irradiation of multiwalled carbon nanotubes: The effect on failure by inner tube sliding. *Phys. Rev. B* 2006; 73: 224106.
9. Morgan P. Carbon fiber and their material composites. CRC Press, USA; 2005.
10. Telling GH, Ewels CP, Ahlam A, Malcolm IH. Wigner defects bridge the graphite gap. *Nature Materials*. 2003; 1-5.
11. Evora MC, Klosterman, Lafdi D K, Li L, Abot .L. Functionalization of carbon nanofibers through electronbeam irradiation. *Carbon* 2010;48: 2037-46.

12. Zou H, Yang Y, Li Q, Zhang J, Liu Z. Electron beam- induced structure transformation of single-walled carbon nanotubes. *Carbon* 2002; 40: 2263-84.
13. Wang ZL, Kang, ZC. Pairing of pentagon and hexagon carbon rings in the growth of nanosized carbon spheres synthesized by a mixed-valent oxide-catalytic carbonization process. *J. Phys. Chem.* 1996; 100: 17725-31.
14. Zhang X, Sreekumar T V, Liu T, and Kumar S. Properties and Structure of Nitric Acid Oxidized Single Wall Carbon Nanotube Films. *J. Phys. Chem. B.* 2004; 108: 16435-40.
15. Endo M, KimYA, Hayashi T, Yanagisawa T, Muramatsu H, Ezaka M, Terrones H, Terrones M, Dresselhaus M.S. Microstructural changes induced in stacked cup carbon nanofibers by heat treatment. *Carbon* 2003; 41:1941-47.
16. Zickler GA, Smarsly B, Gierlinger N, Peterlik H, Paris O. A reconsideration of the relationship between the crystallite size L_a of carbons by X-ray diffraction and Raman spectroscopy. *Carbon* 2006; 44:3239-46.
17. Saikia BK, Boruah RK, Gogoi PK. A X-ray diffraction analysis on graphene layers of Assam coal. *J. Chem. Sci.* 2009; 121, 1: 103–6.
18. Hussain R, Qadeer R, Ahmad M, Saleem M. X-ray diffraction study of heat-treated graphitized and ungraphitized carbon. *Turk J Chem.* 2000; 24: 177-183.
19. Li ZQ, Lu CJ, Xia, ZP, Zhou Y, Luo Z. X ray diffraction patterns of graphite and turbostratic carbon. *Carbon* 2007; 45: 1686-95.